Discharge Estimation by the Aid of Isovel Contours in a Tidal River with Partially Reverse Flow

M. Givehchi[1], M. F. Maghrebi [2,*], K. Kawanisi[3]

Received: March 2008, Accepted: March 2009

Abstract: *Maghrebi has previously introduced a model for the production of isovel contours in a normalized form, which can be used for estimation of discharge in artificial and natural channels. The model is applied to a tidal river with partially reverse flow, which is caused by opening a sluice gate located asymmetrically close to the right bank of the Ohta floodway in Hiroshima, Japan. An acoustic Doppler current profiler (aDcp) was used to measure the velocity profiles at different verticals and then discharge was calculated. In addition, the estimated discharge based on each measured point and the predicted isovels of flow cross section was obtained. The results show that the corresponding errors for the measured points away from the solid boundaries and the imaginary boundary of the flow between the two adjacent regions with opposite directions, which are associated with lower absolute values of isovels, are reasonable.*

Keywords: *Discharge estimation, aDcp, Isovel contours, Reverse flow, Tidal river.*

1. Introduction

The difficulties of understanding the instantaneous flow characteristics in tidal rivers are mainly associated with the conventional invasive instruments, expense and considerable time consumption [1]. Discharge measurement in tidal rivers has to be completed quickly, due to the fact that flow conditions vary rapidly. The flow in tidal estuaries is three dimensional and very complicated which is particularly due to tidal oscillations associated with changes in depth, mean velocity, direction of flow, and density gradients affected by salt, heat and suspended particles. Estimation of discharge in a tidal river is one of the significant issues of flood management. The problem originates from the boundaries, where the flow is almost stagnant. The boundaries are recognized as two types: solid boundary and imaginary boundary between two adjacent regions with opposite directions of flow. It has always been difficult to estimate some quantities close to zero, and velocity is not an exception. Therefore, this will affect the discharge estimation.

The time variations of water stage and discharge have shown that during ebb and flood flows the sign of discharge Q will be positive and negative, respectively [1-2]. The general form of stage discharge is a looped curve. In other words, at a certain time the sign of discharge will be positive or negative. However, the complexity of flow is much higher in a tidal stream with partially reverse flow because in this case, at any time two different regions of flow with positive and negative signs can be discerned. Therefore, to deal with such a complex flow two kinds of tasks should be carried out. The field measurements should be conducted by a rapid, accurate and multi-point measurement instrument such as an aDcp (acoustic Doppler current profiler). Data processing is the other task. A method, which works with a few number of velocity measurements, is required. Maghrebi [3] has proposed the method of single point measurement for discharge estimation. A combination of these two will be able to solve the complicated flow problems such as a tidal flow with partially reverse flow. The objective of this paper is application of the single point measurement in discharge estimation of the instantaneous flow in a tidal river with partially reverse flow.

* *Corresponding Author: Email: Maghrebi@ferdowsi.um.ac.ir*

1 *Ph.D. student, Department of Civil Engineering, Ferdowsi University of Mashhad, Iran.*

2 *Associate Professor, Department of Civil Engineering, Ferdowsi University of Mashhad, Iran.*

3 *Associate Professor, Department of Civil and Environmental Engineering, Graduate School of Engineering, Hiroshima University, Kagamiyama 1-4-1, Higashi Hiroshima, Japan.; E-mail: kiyosi@hiroshima-u.ac.jp*

2. Cross sectional isovel contours

The proposed method is able to predict the normalized isovel contours at the cross sections of straight ducts and irregular open channels with different roughness and geometry [4-5]. As shown in Figure (1), it is assumed that each element of boundary (ds) influences the velocity at an arbitrary point (M) on the cross section:

$$\mathrm{du} = f(\mathbf{r}) \times c_1 \, \mathbf{ds} \tag{1}$$

where du is the velocity deviation due to a boundary element like ds at point M in the cross section of flow, f (r) is a velocity function which is similar to the dominant velocity profile over a flat plate with infinite width, r is a positional vector (starting at a boundary element and ending at the considered point in the flow section- Figure 1) and c_1 is a constant related the boundary roughness. The boundary is to be divided into short elements of length ds where each element is a vector along the wetted perimeter while moving from the left bank toward the right bank.

Then, the total effect of boundary can be obtained by integration along the wetted

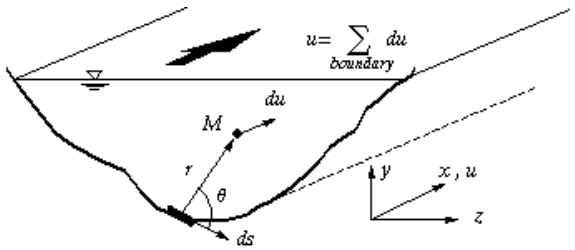

Fig. 1 The effect of a boundary element on the velocity of a point like M, in a river section

perimeter. It is computed as:

$$\mathrm{u} = \int_{boundary} c_1 \, f(\mathbf{r}) \times \mathbf{ds} \tag{2}$$

where u is the streamwise velocity vector at a point on the channel section. The vector direction of velocity on the left hand side of Equation (2) is the same as the vector product of r × ds on the right hand side, which is a normal to flow section towards downstream with a magnitude of $r.ds.\sin\theta$. So from Equation (2) we have:

$$u = \int_{boundary} c_1 \, f(r) \; \mathrm{d}s \; \sin\theta \tag{3}$$

where θ is the angle between the positional vector (starting at a boundary element and ending at the considered point in the flow section) and the boundary elemental vector and r is a radial distance. *f(r)* is replaced by a power law relationship that is commonly used to fit velocity profile in closed conduits and open channels [6]. It follows that:

$$f(r) = u_* \, c_2 \, r^{\frac{1}{m}} \tag{4}$$

where c_2 is a constant related to the nature of flow, and $u_* = \sqrt{\tau_0 / \rho}$ is the boundary shear velocity, where τ_0 is the boundary shear stress and ρ is the mass density of fluid. By replacing *f(r)* from Equation (4) into Equation (3), the local point velocity at an arbitrary position in the channel section like *M* in Figure (1), *u(z, y)*, is obtained as:

$$u(z,y) = \int_{boundary} c_1 \, c_2 \sin\theta \; u_* \, r^{1/m} \, \mathrm{d}s \tag{5}$$

The exponent *m* usually ranges between 4 and 12 depending on the intensity of turbulence [6]. However, the sixth root of power law profile has been found to be equal to the Manning's formula, which can be well applied to the natural streams i.e. *m* = 6 [7]. The average velocity is then given by continuity as:

$$V = \frac{1}{A} \int_A \left(\int_{boundary} c_1 \, c_2 \sin\theta \; u_* \, r^{1/m} \, \mathrm{d}s \right) \mathrm{d}A \tag{6}$$

Finally, by using the mean cross-sectional velocity *V*, the normalized point velocity $\tilde{U}$(z, y), is given by:

$$\tilde{U}(z,y) = \frac{u(z,y)}{V} = \frac{\int_{boundary} c_1 \, c_2 \sin\theta \; u_* \, r^{1/m} \, \mathrm{d}s}{\frac{1}{A} \int_A \left(\int_{boundary} c_1 \, c_2 \sin\theta \; u_* \, r^{1/m} \, \mathrm{d}s \right) \mathrm{d}A} \tag{7}$$

Equation (7) provides the normalized velocity at a point as a function of the boundary geometry and relative roughness. An advantage of the Maghrebi's model is that it allows the

consideration of the hydraulic characteristics of the boundary and their influences on the flow.

3. Study site and instrument description

The Ohta River is divided into six branches before discharging to Hiroshima Bay. Gion diversion channel is a branch of Ohta River (Figure 2a). At the Gion Bridge location, to control the flow, three sluice gates are installed between the piers. Two gates on the left and the center are closed. Downstream of the gate, the recirculation zone is formed (Figure 2b). The freshwater runoff from the right gate, which is located at about 9 km upstream from the mouth, is limited by fixing the gate opening at a height of 0.3 m from the bottom. The observation site, which is located at 96 m downstream of the Gion gate, is shown in Figure 2(b). Due to unsteadiness of flow in tidal rivers, a rapid velocity measurement across a wide river is essential. To overcome the difficulties of rapid measurements, an aDcp was used to measure accurate vertical profiles of mean velocities. The aDcp belongs to a class of acoustic current profilers usually referred to an incoherent Doppler profiler [8-10]. The aDcp is operating at 2.0 MHz and 23 Hz pinging rate. The three transducers, which are equally spaced at 120° azimuth angles, generate a beam oriented 25° off the vertical axis. Using a compass and a two-axis tilt sensor, the beam Doppler velocities are transformed into earth coordinates by an internal processor. The aDcp allows one to measure the currents and acoustic scattering strength in depth cell sizes of 0.03 m [2]. The directions of aDcp axes (the x, y and z axes) are based on the definition of a right-handed coordinate system. The x axis shows the main stream direction, and the streamwise velocity, u, is positive during the flood and negative during the ebb. The vertical axis, y, originates at the bottom and points upward. The water depth was measured using a pressure transducer of aDcp.

The bed profile is plotted in Figure 2(c). The top width of the river at the observation site is about 130 m and the maximum depth of water is 2.68 m, which is located at a distance of 62 m from the left bank of the river. The shear stress distribution which is used to produce the isovel contours from Equation (7) is also shown in this figure. When the model is applied to a partially reverse flow, it should be noted that on the bed region where the flow occurs in opposite directions, the sign of shear stress, which is affected by the direction of velocity vector, will be changed. According to the field velocity profile the shear stress distribution along the wetted perimeter is considered as shown in Figure 2(c). Reverse flow occurs on the left part of the river bed, so the sign of shear stress is negative. On the right boundary as the flow is directed toward downstream, the shear stress has a positive sign.

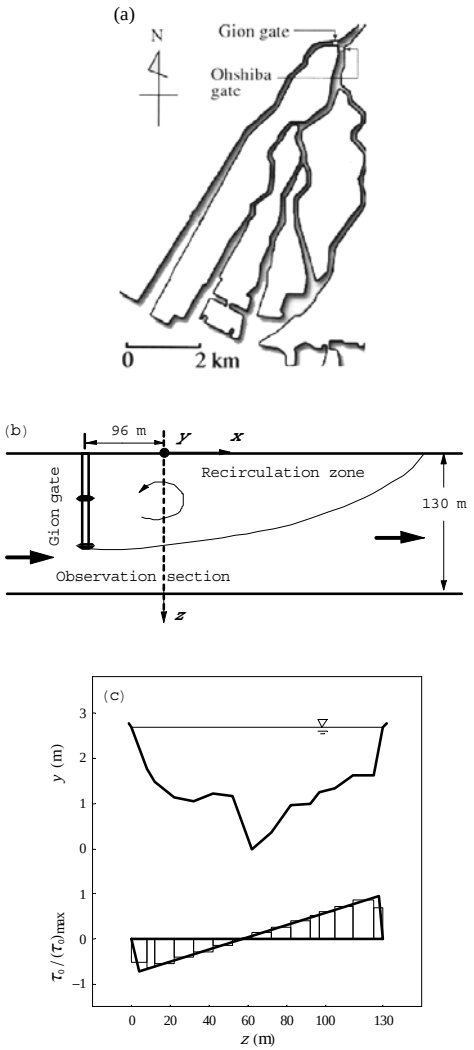

Fig. 2 (a) Ohta estuary, (b) plan view of the observation section and (c) observation section of the river bed profile at the immediate downstream of the Gion gate with a simplified shear stress distribution

The points of zero shear stress are assumed to be coincided with the left and right banks as well as the stagnant region, which is located at an approximate distance of 57 m from the left bank. Then a linear shear stress distribution is applied to the boundary Figure 2(c). The positive shear stresses are occurred on the right half of the bed profile where the sluice gate is opened and negative values are assumed to occur on the left. The corresponded relative values of the shear stresses for each segment of the wetted perimeter on the bed from left to right are -0.52, -0.63, -0.54, -0.40, -0.27, -0.13, 0, 0.14, 0.28, 0.42, 0.52, 0.61, 0.72, 0.86 and 0.72 (Figure 2c).

4. Discharge estimation

The discharge can hardly be measured directly and is usually calculated from a stage-discharge curve, derived from gauging station records [11]. Enough discharge measurements during rises and consequent recessions must be made at the gauging station to calibrate the parameters and to check on the computed discharge, which is a time consuming task. On the other hand, the flow conditions of tidal streams are rarely steady or uniform. It make stage discharge relations complex. In addition, the accuracy of stage-discharge curves will be questionable as the hydraulic characteristics of river are changing gradually. Therefore, to have a reliable estimation of discharge, direct measurements are needed.

In order to float the instrument on the water surface, it was placed on a flat and light plate. The supporting system was formed in a streamlined shape to minimize the drag and disturbance (Figure 3a). Then a piece of rope was used to move the probe across the river section manually (Figure 3). The preferred method of measuring discharge in a large tidally affected stream is the moving boat method [12-13]. At each transverse location, the probe was remained stationary for duration of 60 s to collect the instantaneous velocity at a sampling rate of 23 Hz.

The measured discharge Q_a , at a river section is estimated as the summation of the product of point velocity multiplied by the representative area over the entire section, which is called actual discharge. Accordingly, the velocities are measured at different verticals with the transverse

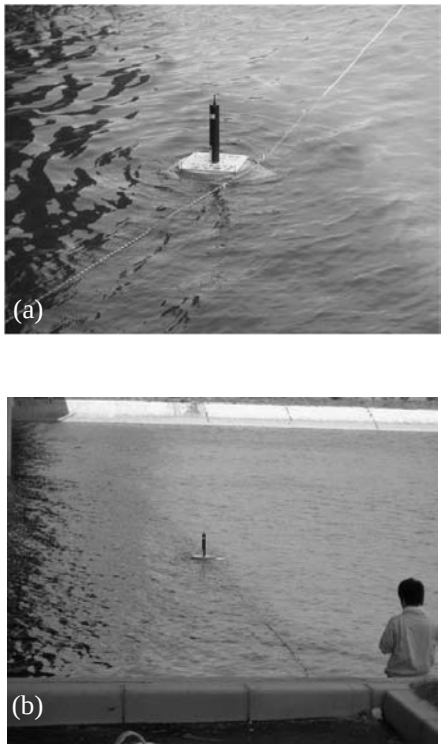

Fig. 3 Moving aDcp across the Gion diversion channel using a piece of rope (a) a close view and (b) a far view

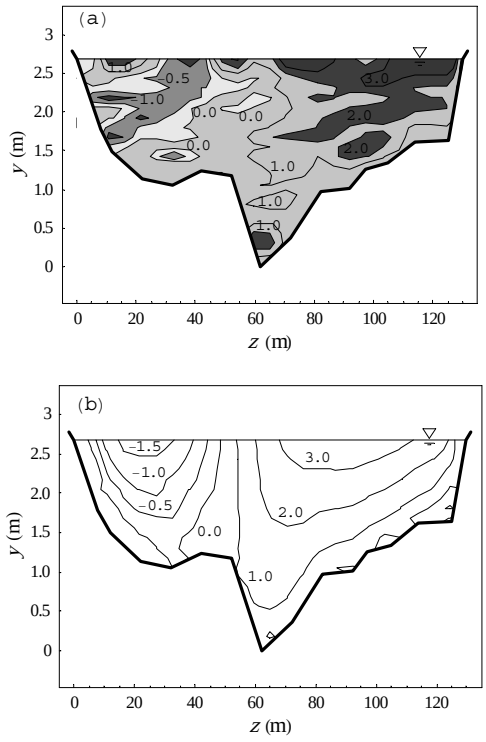

Fig. 4 Isovel counters at the observation section of the Gion River based on (a) field data (b) Maghrebi's model

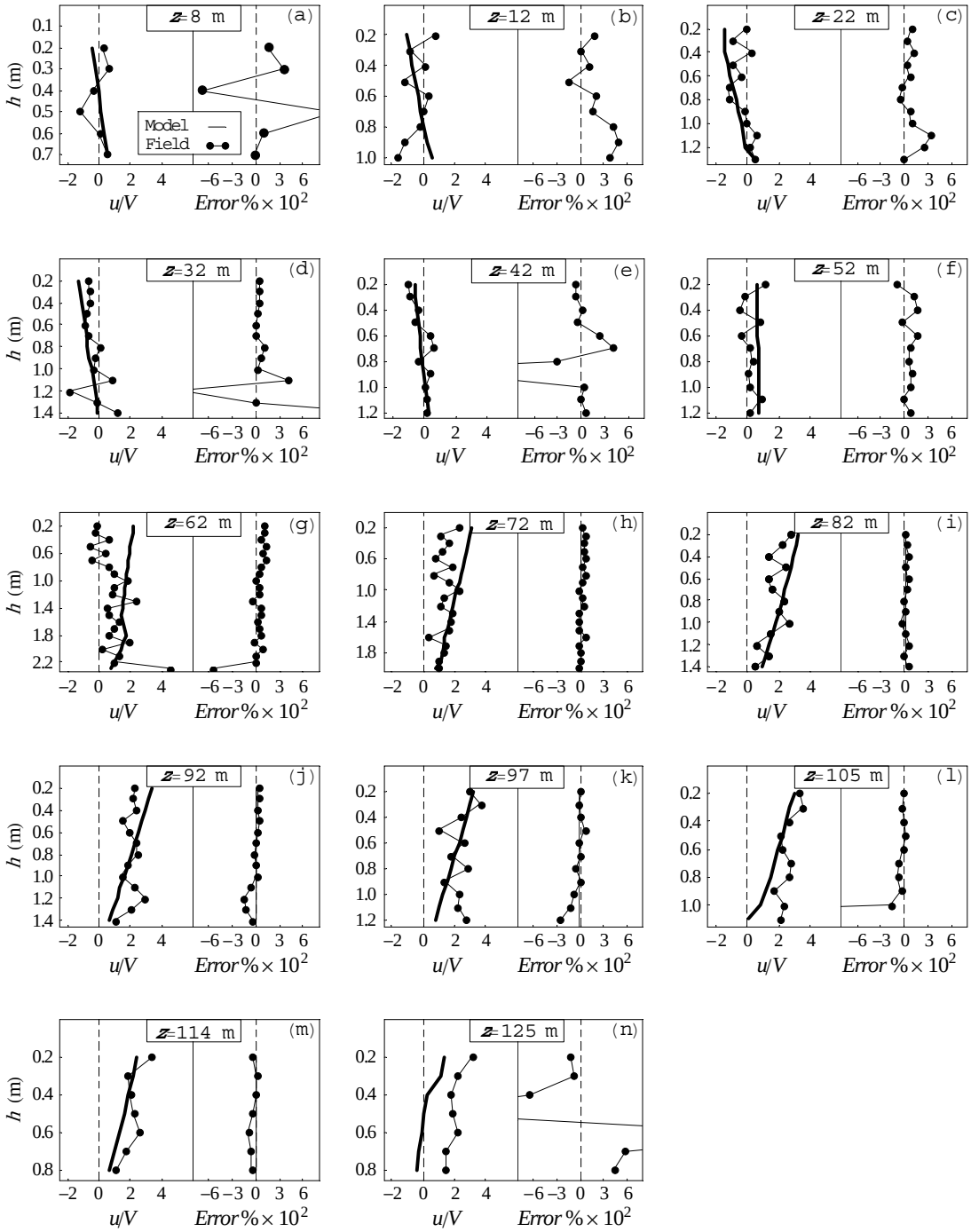

Fig. 5 Measured velocity profiles using aDcp in comparison with the results provided by the proposed model at different transverse verticals of the observation section and the corresponded errors

distances of 8, 12, 22, 32, 42, 52, 82, 92, 97, 105, 114 and 125 meters from the left bank. The cross sectional area of the river and the average velocity are computed as 194.06 m^2 and 10.7 cm/s, respectively. The corresponded discharge is 20.76 m^3/s.

The isovel contours in Figure 4(a) are calculated based on the field data. As shown, the direction of the velocity at the left part of the river section is headed towards upstream, while the flow on the right part flows downstream. Figure 4(b) shows the predicted isovel contours calculated based on the proposed model [3].

Despite large fluctuations of the measured

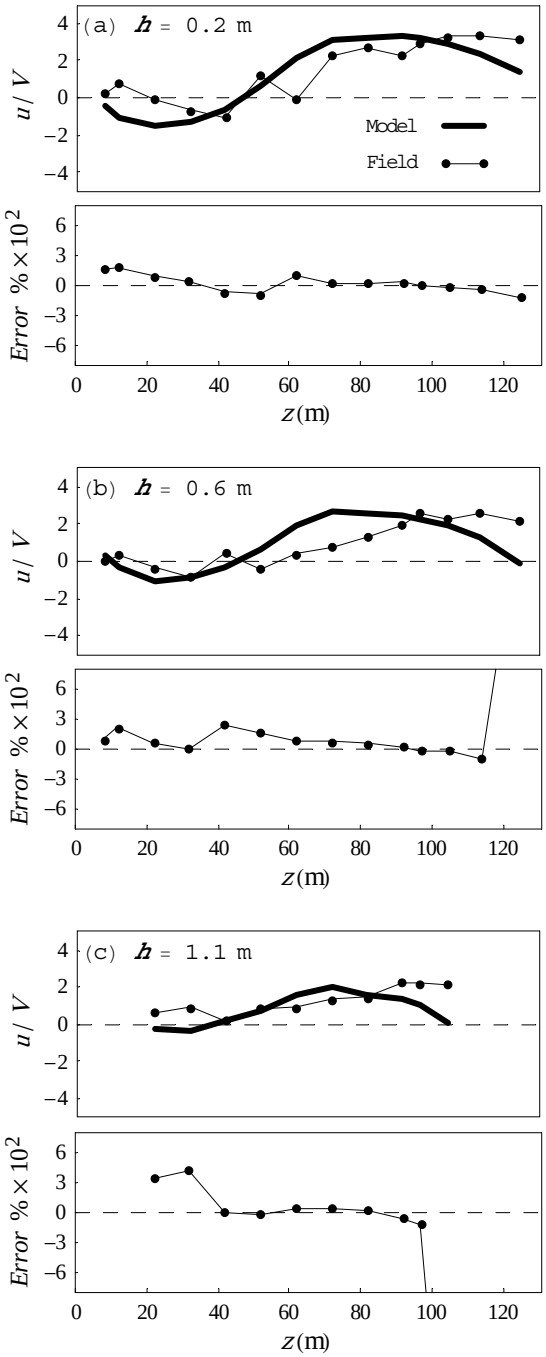

Fig. 6 Measured velocity profiles using aDcp in comparison with the results provided by the proposed model at different transverse horizontal stripes of the observation section and the magnitude of errors

velocity, a fairly good qualitative agreement can be observed between the isovel contours produced by the experimental data and model. Determination of the roughness coefficients in natural rivers is a difficult task. In this study the roughness of river boundary over each segment of the cross-section is assumed to be uniform.

Figure (5) shows the measured velocity profiles at different verticals with solid circles connected to each other with broken lines. Positive sign for velocity shows that the direction of flow is towards downstream and the negative sign refers to the opposite direction. Due to the probe limitations, velocity could not be measured at a vertical distance of less than 0.2 m from the water surface and 0.1 m depth of water from the bottom of the river.

In addition, velocity profiles according to the proposed model, which are shown with thick solid lines, are plotted against the field data (Figure 5). Close to the left and right walls of the river, larger differences between the predicted velocity profile and the measured data can be observed. Estimation of discharge is carried out by the use of a single point of velocity measurement in combination with the isovel contours produced by the proposed model [3].

The magnitude of normalized corresponding isovel contour passing through a given measured point can be found. The measured velocity at a point in channel cross section is *u(z,y)* and the magnitude of the normalized corresponding isovel contour is $\tilde{U}(z, y)$, then the total discharge can be obtained by:

$$Q_c = A \times \frac{u(z,y)}{\tilde{U}(z,y)} \tag{8}$$

where Q_c is the total calculated discharge passing through the cross sectional area A and $\tilde{U}(z, y) = u(z,y)/V$. The relative percentage of error in discharge estimation is calculated by:

$$Error\ \% = \frac{Q_a - Q_c}{Q_a} \times 100 \tag{9}$$

In Figure (5), the associated errors corresponded with the measured velocity points, are shown. It is clear that when the normalized isovel contours are close to zero, the estimated discharges by the use of Equation (8) will approach infinity. These points are near the river bed (Figures 5g and 5l), river sides (Figures 5a and 5n), and isovel contours with extremely small magnitude (Figures 5d- e) that usually exist in tidal rivers.

Figure (6) shows the measured velocity

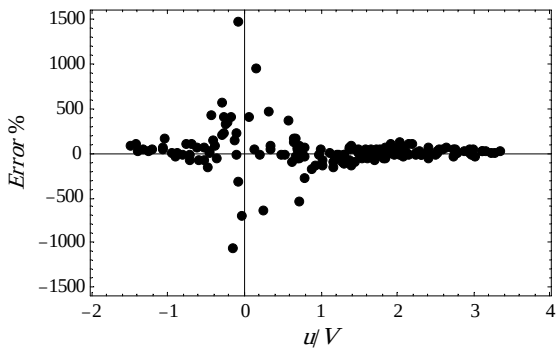

Fig. 7 Variation of error as a function of u/V

profiles at different horizontals with solid circles connected to each other with broken lines. The water depths are 0.2, 0.6 and 1.1 m. Also, velocity profiles according to the proposed model, which are shown with thick solid lines, are plotted against the field data. On the lower part of the figure, the relative percentage of error in discharge estimation, corresponded with each measured point, is shown. Due to the velocity fluctuations in a vertical, if the discharge is estimated based on a single point of velocity measurement, the result will be far from the actual discharge.

It is interesting to observe the error distribution as a function of *u/V*. Figure (7) shows the results for all 164 points. As expected, by approaching *u/V* towards zero, the magnitude of the associated errors, are increased. However, for larger values of $|u/V|$, the magnitude of errors are decreased.

In Table 1, for a number of given ranges of *u/V*, the number of the measured points and corresponded errors of average discharge estimations are given. It is observed that for $u/V<-0.5$ and for $u/V>0.5$, the magnitude of errors are decreased drastically in comparison with the range of $-0.5<u/V<0.5$. This is in accordance with the previously observed results [3].

To minimize the uncertainty, it is recommended to estimate the discharge using a number of measured velocity points. Although any combination of the measured points can be used for the estimation of discharge, two ways of grouping are chosen. The first one, which is shown in Figure 8(a), seems to the most reasonable grouping technique, because the points in a vertical are measured simultaneously.

Table 1 Error of average discharge estimation

u/V	No. of points	Error of average discharge %
-1.5 to -1.0	9	73.71
-1.0 to -0.5	12	13.20
-0.5 to 0.0	22	239.75
0.0 to 0.5	12	-557.96
0.5 to 1.0	22	-4.88
1.0 to 1.5	21	-28.31
1.5 to 2.0	25	10.28
2.0 to 2.5	19	27.78
2.5 to 3.0	16	29.28
3.0 to 3.5	6	23.56

Based on each point in a group an estimated discharge is obtained. In all cases, the best expected value of discharge will be the mean value. For each column, the number of points contributed in the calculation of the error of average discharge, are given in Table 2. The best results are related to C14 and C9 with 16.8 % and 19.3 % of errors, respectively. C14 is near the right wall and C9 is corresponded with the highest velocities at the river cross section.

A big difference can be observed between the real and estimated velocities near the side of the river and on the left part of the section. Therefore, the corresponded errors in discharge estimation are relatively large. It has been mentioned that as the corresponding values of the contour lines are increased, errors in discharge estimations will be decreased [3].

The second considered grouping technique for the measured points are shown in Figure 8(b). These are essentially horizontal arrangements. In Table 3, the error of average discharge calculated for this type of grouping are presented. The number of horizontal groups reaches to 22. The maximum and minimum numbers of measured points contributed in averaging technique are 14 and 1, respectively. Unlike the results of vertical grouping (Table 2), the results of horizontal grouping provide a better estimation of discharge (Table 3). Although the measured points in a row are not synchronized and this is one of the sources of error, surprisingly better estimations of

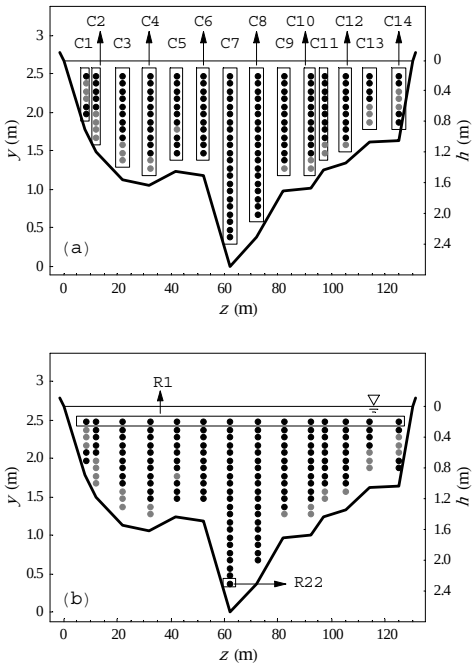

Fig. 8 Definition areas for calculation of the error of average discharge estimation (a) vertical groups (b) horizontal groups

average discharges are obtained. The main reason for this behavior is higher values of the corresponded isovel contours. The other reason is oscillation of the measured velocity with almost a constant magnitude about the theoretical isovel values.

By discarding some of the points associated with low values of isovel contours, which are shown by gray dots in Figure (8), the error of average discharge estimation are generally decreased (case 2 in Tables 2 and 3). For example, by discarding some of the points in columns C1-C6 and C9-C13 and rows R2-R5, R8-R10 and R12 and R13 the errors of average discharge are decreased. The average error of all the measured points (164 points) is -0.6% and by removing the points associated with low values of isovel contours (25 points), error of average discharge will reach to 22%. This is mainly due to the summation of large errors with a number of small errors with opposite signs.

According to Equation (5), the normalized velocity distributions are sensitive to boundary shear stress distributions. Figure (9) shows three more distributions for the boundary shear stresses as well as the errors of average discharges. By

Table 2 Errors of average discharge estimation by using vertical groups (Figure 8a)

Vertical Groups	z [m]	No. of Points (Case 1)	Error of average discharge % (Case 1)	No. of Points (Case 2)	Error of average discharge % (Case 2)
C1	8	6	145.3	3	81.6
C2	12	9	199.9	5	72.8
C3	22	12	81.9	9	45.2
C4	32	13	92.9	11	-25
C5	42	11	-161.2	10	25.8
C6	52	11	64	11	64
C7	62	22	23.6	22	23.6
C8	72	19	25.3	19	25.3
C9	82	13	19.3	12	17
C10	92	13	-20.3	11	-7.8
C11	97	11	-40.2	9	-7.2
C12	105	10	-406.3	9	-46.4
C13	114	7	-42.5	4	-18
C14	125	7	16.8	4	198.7

Table 3 Errors of average discharge estimation using horizontal groups (Figure 8b)

Horizontal Groups	h [m]	No. of Points (Case 1)	Error of average discharge % (Case 1)	No. of Points (Case 2)	Error of average discharge % (Case 2)
R1	0.2	14	24.2	14	24.2
R2	0.3	14	44.8	13	20.7
R3	0.4	14	-48.9	12	54.8
R4	0.5	14	-98.1	12	6.5
R5	0.6	14	232.1	12	80
R6	0.7	14	88	12	96.1
R7	0.8	13	42.2	11	16.6
R8	0.9	11	-115.5	9	30.7
R9	1.0	11	30.1	10	-4.8
R10	1.1	10	-300.6	7	59.1
R11	1.2	9	-105.6	7	-132.9
R12	1.3	6	-37.4	3	-25.3
R13	1.4	5	308.9	2	26.4
R14	1.5	2	22.7	2	22.7
R15	1.6	2	44.7	2	44.7
R16	1.7	2	16.4	2	16.4
R17	1.8	2	31.7	2	31.7
R18	1.9	2	-4.5	2	-4.5
R19	2.0	2	29.7	2	29.7
R20	2.1	1	-10.2	1	-10.2
R21	2.2	1	-2.9	1	-2.9
R22	2.3	1	-536.1	1	-536.1

considering a constant shear stress on bed and zero shear stress on sides, the error of average discharge is 7.6 % (Fig. 9a). Error is increased to 17.7 % when uniform shear stress distribution is considered (Figure 9b). Linear shear stress distribution with its maximum values at the river banks is accompanied with a larger error of 115.4

Fig. 9 Different assumptions for shear stress distributions

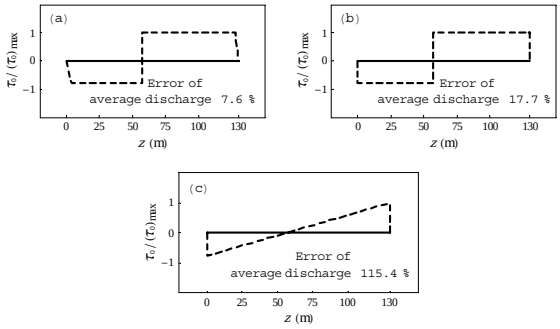

% (Figure 9c). The only difference between this and the one, which is used in this paper (see Figure 2c), is the shear stress distribution on the sides of river. It is clear that the shear stress distribution, which is shown in Figure 9(c), in comparison with Figure 2(c), provides larger error. This shows the sensitivity of the model to the shear stress distribution.

5. Conclusions

In large tidal rivers with partially reverse flow the task of velocity measurement should be completed quickly. This is due to high unsteadiness of the flow. This maybe fulfilled using an aDcp. Due to the fluctuations of the measured velocities, it is understood that discharge estimation based on a number of measured points would lead to more appropriate results.

A combination of a rapid velocity measurement technique and a theoretical approach for estimation of discharge based on minimum number of points of velocity measurements can be considered as an effective way to undertake the task of discharge estimation. Although no field measurement for estimation of shear stress distribution along the wetted perimeter of the river section, which is needed to be applied in the proposed model, has been performed, a linear shear stress distribution for complicated circumstances of a tidal river with partially reverse flow seems to be a reasonable assumption.

Discharge estimation for each point of velocity measurement is possible. However, due to large fluctuations in the measurements, large errors will be expected. Therefore, discharge estimation based on a set of points instead of a single point will be closer to the actual discharge. The results of this study have revealed that the proposed model for estimation of discharge using a single point of velocimetry can be considered as an appropriate, fast and easy model for the production of isovel contours in natural rivers with partially reverse flow. When using a single point of velocity measurement for estimation of discharge, if the related normalized contour values are small, the corresponding errors will be large. Therefore, it is generally proposed to select the measured points from the regions with the corresponding high values of isovels in the range of u/V<-0.5 and u/V>0.5. It is also suggested that estimation of discharge using horizontal groupings of the points leads to lower magnitude of error in comparison with the vertical groupings.

References

[1] Chen, Y.C., Chiu, C.L.: 2002, An efficient method of discharge measurement in tidal streams, J. of Hydrology, 265, 212-224.

[2] Kawanisi, K.: 2004, Structure of turbulent flow in a shallow tidal estuary, J. of Hydraulic Eng., ASCE, 130(4), 360-370.

[3] Maghrebi, M.F.: 2006, Application of the single point measurement in discharge estimation, J. Advances in Water Resources, 29, 1504-1514.

[4] Maghrebi, M.F., Rahimpour, M.: 2005, A simple model for estimation of dimensionless isovel contours in open channels, J. of Flow Measurement and Instrumentation, 17, 347-352.

[5] Maghrebi, M.F., Ball, J.E.: 2006, New method for estimation of discharge, J. of Hydraulic Eng., ASCE, 132(10), 1044-1051.

[6] Yen, B.C.: 2002, Open channel flow resistance, J. of Hydraulic Eng., ASCE, 128(1), 20–39.

[7] Chen, C.L.: 1991, Unified theory on power laws for flow resistance, J. of Hydraulic Eng., ASCE, 117 (3), 371-389.

[8] Lhermitte, R., Serafin, R.: 1984, Pulse-to-pulse coherent Doppler sonar signal processing techniques, J. Atmos. Ocean. Technol., 1(4), 293-308.

[9] Verson, F., Melville, W. K.: 1999, Pulse-to-pulse coherent Doppler measurements of waves and turbulence, J. Atmos. Ocean. Technol., 16, 1580-1597.

[10] Zedel, L., Hay, A. E., Cebrera, R., Lohrmann, A.: 1996, Performance of a single-beam pulse-to-pulse coherent Doppler profiler, IEEE J. Ocean. Eng., 21(3), 290-297.

[11] Sulzer, S., Rutschmann, P., Kinzelbach, W.: 2002, Flood discharge prediction using two-dimensional inverse modeling, J. of Hydraulic Eng., ASCE, 128(1), 46-54.

[12] Rantz, S.E.: 1983, Measurement and computation of stream flow, Volume 2, Computation of Discharge. US Geology Survey, Water Supply, Paper 2175, US Government Printing Office, Washington.

[13] International Organization for Standardization: 1979, Measurement of liquid flow in open channels–moving boat method, Ref. No. ISO4369-1979(E), Geneva, Switzerland.

Notation

A = cross sectional area of the stream
c_1, c_2 = constants related to the boundary roughness and flow regime, respectively
ds = vector notation along the wetted perimeter
$f(\mathbf{r})$ = velocity function
h = local depth of flow
m = denominator in exponent of the power-law velocity distribution
Q = discharge
Q_a = measured discharge
Q_c = calculated discharge
r = radial distance
$\mathbf{r}$ = positional vector
$\mathbf{u}$ = streamwise velocity vector at a point in the channel section
u = streamwise velocity at a point in the channel section
u_* = shear velocity
$\tilde{U}(z, y)$ = normalized point velocity
V = mean cross sectional velocity
x = streamwise direction
y = vertical direction
z = lateral coordinate measured from the left bank of the stream
τ_0 = boundary shear stress
ρ = mass density
θ = angle between the positional vector and the boundary elemental vector